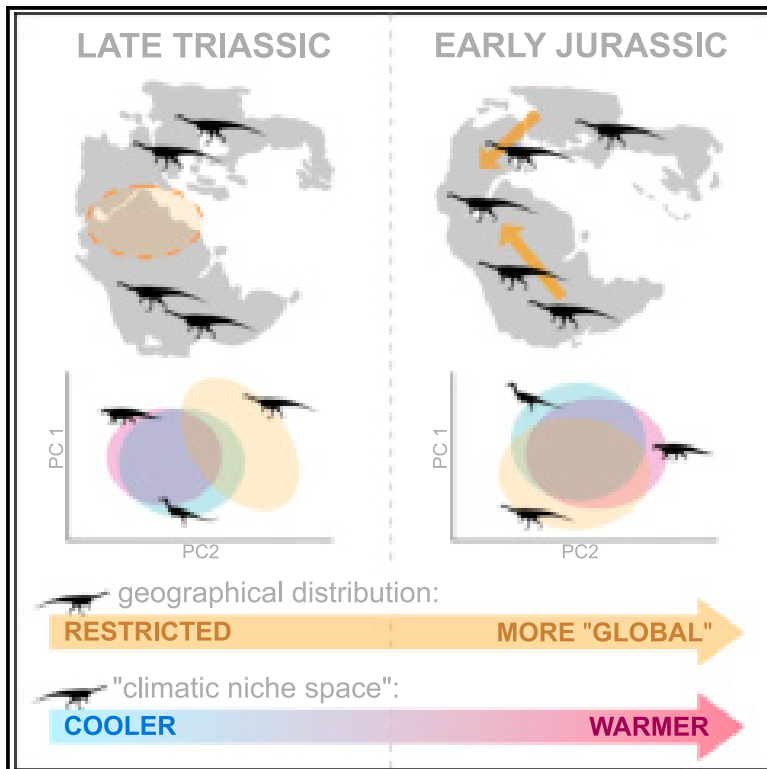


# Current Biology

## Climatic controls on the ecological ascendancy of dinosaurs

### Graphical abstract



### Authors

Emma M. Dunne,  
Alexander Farnsworth,  
Roger B.J. Benson, ..., Paul J. Valdes,  
Daniel J. Lunt, Richard J. Butler

### Correspondence

dunne.emma.m@gmail.com

### In brief

During their early evolution, sauropodomorph dinosaurs were excluded from the hottest, low-latitude climate zones. Dunne et al. show that the geographic expansion of sauropodomorphs after the end-Triassic mass extinction was facilitated by climatic change, supporting the key role of climate in the ascendancy of dinosaurs.

### Highlights

- Early diverging sauropodomorphs were characterized by a cooler climatic niche
- Later in the Early Jurassic, sauropodomorphs shifted to warmer niches
- This shift towards warmer climatic niches occurred during the origin of the Sauropoda
- The global abundance of sauropodomorph dinosaurs was facilitated by climatic change

Report

# Climatic controls on the ecological ascendancy of dinosaurs

Emma M. Dunne,<sup>1,2,8,15,16,\*</sup> Alexander Farnsworth,<sup>3,4,13,14</sup> Roger B.J. Benson,<sup>5</sup> Pedro L. Godoy,<sup>6,7,10,14</sup> Sarah E. Greene,<sup>1,9,12</sup> Paul J. Valdes,<sup>3</sup> Daniel J. Lunt,<sup>3</sup> and Richard J. Butler<sup>1,11,12</sup>

<sup>1</sup>School of Geography, Earth & Environmental Sciences, University of Birmingham, Edgbaston, Birmingham, B15 2TT, UK

<sup>2</sup>School of Geographical Sciences, University of Bristol, University Rd, Bristol, BS8 1SS, UK

<sup>3</sup>State Key Laboratory of Tibetan Plateau Earth System, Resources and Environment (TPESRE), Institute of Tibetan Plateau Research, Chinese Academy of Sciences, Lincui Road, Chaoyang District, Beijing 100101, China

<sup>4</sup>Department of Earth Sciences, University of Oxford, South Parks Rd, Oxford, OX1 3AN, UK

<sup>5</sup>Department of Biology, Universidade de São Paulo, Ribeirão Preto, São Paulo 14040-901, Brazil

<sup>6</sup>Department of Anatomical Sciences, Stony Brook University, 100 Nicolls Rd, Stony Brook, NY 11794, USA

<sup>7</sup>Current address: GeoZentrum Nordbayern, Friedrich-Alexander University Erlangen-Nürnberg (FAU), 91054 Erlangen, Germany

<sup>8</sup>Twitter: @emmadnn

<sup>9</sup>Twitter: @carbonatefan

<sup>10</sup>Twitter: @ButlerLabBham

<sup>11</sup>Twitter: @PedroLGodoy

<sup>12</sup>Twitter: @Palaeo\_Bham

<sup>13</sup>Twitter: @Climate\_AlexF

<sup>14</sup>Twitter: @PaleoLabUSP

<sup>15</sup>Twitter: @palaeoFAU

<sup>16</sup>Lead contact

\*Correspondence: [dunne.emma.m@gmail.com](mailto:dunne.emma.m@gmail.com)

<https://doi.org/10.1016/j.cub.2022.11.064>

## SUMMARY

The ascendancy of dinosaurs to become dominant components of terrestrial ecosystems was a pivotal event in the history of life, yet the drivers of their early evolution and biodiversity are poorly understood.<sup>1–3</sup> During their early diversification in the Late Triassic, dinosaurs were initially rare and geographically restricted, only attaining wider distributions and greater abundance following the end-Triassic mass extinction event.<sup>4–6</sup> This pattern is consistent with an opportunistic expansion model, initiated by the extinction of co-occurring groups such as aetosaurs, rauisuchians, and therapsids.<sup>4,7,8</sup> However, this pattern could instead be a response to changes in global climatic distributions through the Triassic to Jurassic transition, especially given the increasing evidence that climate played a key role in constraining Triassic dinosaur distributions.<sup>7,9–16</sup> Here, we test this hypothesis and elucidate how climate influenced early dinosaur distribution by quantitatively examining changes in dinosaur and tetrapod “climatic niche space” across the Triassic-Jurassic boundary. Statistical analyses show that Late Triassic sauropodomorph dinosaurs occupied a more restricted climatic niche space than other tetrapods and dinosaurs, being excluded from the hottest, low-latitude climate zones. A subsequent, earliest Jurassic expansion of sauropodomorph geographic distribution is linked to the expansion of their preferred climatic conditions. Evolutionary model-fitting analyses provide evidence for an important evolutionary shift from cooler to warmer climatic niches during the origin of Sauropoda. These results are consistent with the hypothesis that global abundance of sauropodomorph dinosaurs was facilitated by climatic change and provide support for the key role of climate in the ascendancy of dinosaurs.

## RESULTS AND DISCUSSION

### Early-dinosaur climatic niche space

Climate variation has long been considered to be a fundamental control on the distribution of land vertebrates during the Triassic, including early dinosaurs, and in particular sauropodomorphs.<sup>9,10,17–20</sup> Most previous examinations of the role of climate have been conducted at the regional scale (e.g., Whiteside et al.,<sup>9</sup> Bernardi et al.,<sup>10</sup> and Mancuso et al.<sup>12</sup>) or based on visual comparisons to previously published maps from general circulation

models of Late Triassic climate (e.g., Brusatte et al.<sup>21</sup>), or they have used paleolatitudinal position as a coarse proxy for climatic conditions (e.g., Ezurra et al.<sup>18</sup>). Our approach builds on this previous work by permitting direct comparison between taxon distributions and climate conditions. We integrated dinosaur occurrence data from the Paleobiology Database ([paleobiodb.org](http://paleobiodb.org)) with paleoclimatic reconstructions from a general circulation model (HadCM3L), allowing characterization of the climatic conditions under which individual species and higher-level taxonomic groups occurred, using a broader range of climatic variables than was

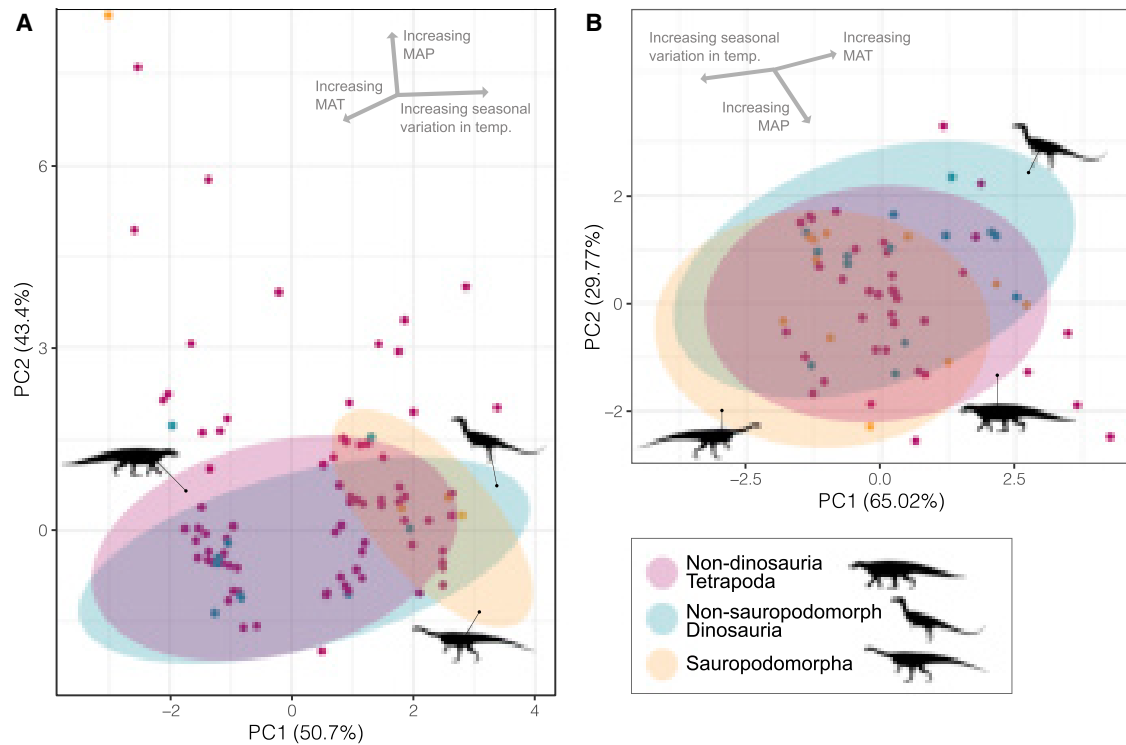


**Figure 1. Climatic niche space across the Triassic-Jurassic boundary**

(A and B) Climatic niche space for non-dinosaur tetrapods (red), non-sauropodomorph dinosaurs (blue), and sauropodomorphs (yellow) in the Late Triassic (A) and Early Jurassic (B). Each point on the plots represents an individual taxonomic occurrence. Ellipses represent 68% confidence intervals based on a PCA of four climate variables (MAT, mean annual precipitation, seasonal variation in temperature, and seasonal variation in precipitation). Silhouettes from [phylopic.org](https://phylopic.org) (see [acknowledgments](#) for creator credits).

previously possible. We quantified climatic niche space for sauropodomorphs, non-sauropodomorph dinosaurs, and other (non-dinosaurian) tetrapods in the Late Triassic and Early Jurassic using a principal component analysis (PCA; [Figure 1](#)). Obtaining information on species' fundamental niches from the fossil record is challenging; therefore, the term "climatic niche" used here refers to an approximation of the realized climatic niche of the fossil taxa (i.e., the set of climatic conditions occupied by a taxon).

During the Late Triassic, climatic niche space for sauropodomorphs was more restricted than for other groups, including both non-dinosaurian tetrapods and non-sauropodomorph dinosaurs (i.e., theropod dinosaurs, given that definite records of Triassic ornithischians remain unknown) ([Figure 1A](#)). Sauropodomorphs favored cooler conditions with higher seasonality in surface temperatures ([Figures 2A](#) and [S1A–S1D](#)). In contrast, Late Triassic theropod dinosaurs occupied a wider climatic niche space than sauropodomorphs ([Figure 1A](#)). Their ranges are more similar to other (non-dinosaur) tetrapods and encompass warm climatic regions with a narrow range in seasonal temperature from which sauropodomorphs were absent ([Figures 2A](#) and [S1A–S1D](#)), although the climatic niche spaces for all three are statistically significantly different from one another (non-parametric multivariate analysis of variance [npMANOVA],  $p < 0.001$ ; [Table S1](#)).

In the Early Jurassic, climatic niche spaces for all three of these groups overlap much more closely ([Figure 1B](#)), although they remain statistically significantly different from one another (npMANOVA,  $p < 0.001$ ; [Table S1](#)). Early Jurassic sauropodomorphs

occur under a broader range of mean annual temperatures (MATs) than during the Late Triassic, including both warmer and cooler areas, and continue to be most abundant in areas with a high seasonal range in temperature ([Figures 2B](#) and [S1E–S1H](#)). Non-sauropodomorph dinosaurs—which now include ornithischians as well as theropods—and non-dinosaurian tetrapods both show shifts towards cooler temperatures, with a high seasonal range in the Early Jurassic when compared with the Late Triassic. Distributions of individual climate variables ([Figure S1](#) and [Table S1](#)) suggest that MAT and seasonal variation in temperature are the main axes differentiating the climatic niche of early sauropodomorphs from those of other dinosaurs and non-dinosaurian tetrapods, highlighting the importance of temperature variation in determining the distribution of early dinosaurs.

This change in climatic niche space across the Triassic to Jurassic transition is also evident when MAT is optimized as a continuous character onto a phylogeny of early dinosaur species ([Figure 3](#)). Notably, sauropodomorphs show multiple independent expansions into warmer regions during the Early Jurassic, as evidenced by the non-sauropodan sauropodomorphs *Sarapasaurus* and *Seitaad*, as well as sauropods such as *Barapasaurus*.

Sauropodomorphs in both the Late Triassic and Early Jurassic had their maximum abundance in regions with very high seasonal variation in temperature (e.g., seasonal variation on the order of 40°C–50°C). Although such temperature fluctuations appear extreme ([Figures S1C](#) and [S1G](#)), they reflect the continental climatic conditions prevalent on the supercontinent Pangea; they

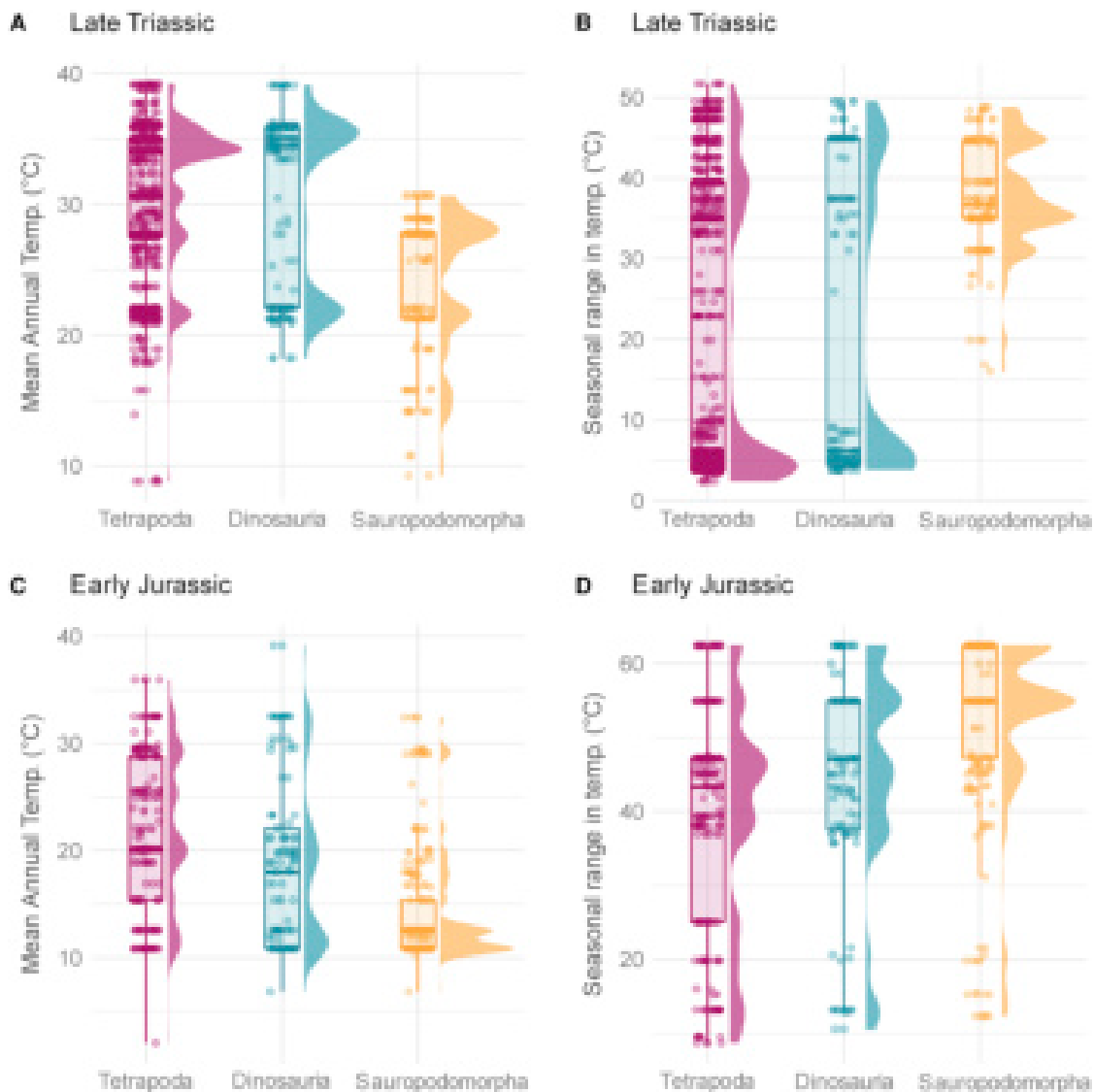


**Figure 2. Ranges of temperature conditions occupied by sauropodomorphs, other dinosaurs, and other tetrapods during the Late Triassic to Early Jurassic**

C(A–D) Raincloud plots displaying ranges of MAT and seasonal range in temperature for non-dinosaur tetrapods (red), non-sauropodomorph dinosaurs (i.e., predominantly theropod dinosaurs for the Late Triassic; blue), and sauropodomorphs (yellow) in the Late Triassic (A and B) and Early Jurassic (C and D). For each group, summary statistics are displayed on a box-and-whisker plot, the raw data as semi-transparent dots, and distribution of these data as a density plot. See also [Figure S1](#) and [Table S1](#).

are also consistent with annual temperature ranges seen in strongly continental climates in the modern day in regions such as the Gobi Desert, where annual temperature ranges can be up to 80°C. The implications of such extreme climatic variation for early dinosaurs and other Triassic tetrapods are worthy of further study.

### Evolutionary model-fitting analysis

Early diverging sauropodomorphs in the Late Triassic were characterized by a cooler climatic niche, while in the Early Jurassic, closer to the later radiation of Sauropoda, they shifted to a warmer niche. To further explore this shift in climatic niche space for sauropodomorphs and non-sauropodomorph

dinosaurs across the Triassic-Jurassic boundary, we conducted an evolutionary model-fitting analysis. This allowed examination of the mode of climatic niche evolution, specifically with regards to MAT, which in previous analyses was a key factor in determining the distribution of early dinosaurs. We accommodated uncertainties in sauropodomorph phylogeny by constructing two alternate topologies for Late Triassic and Early Jurassic sauropodomorph relationships: one following Chapelle et al.<sup>22</sup> and the other following McPhee et al.<sup>23</sup>; however, the results were consistent between these two topologies.

The evolution of sauropodomorph climatic niche space is best explained by a uniform Brownian motion (BM) model (BM1), in

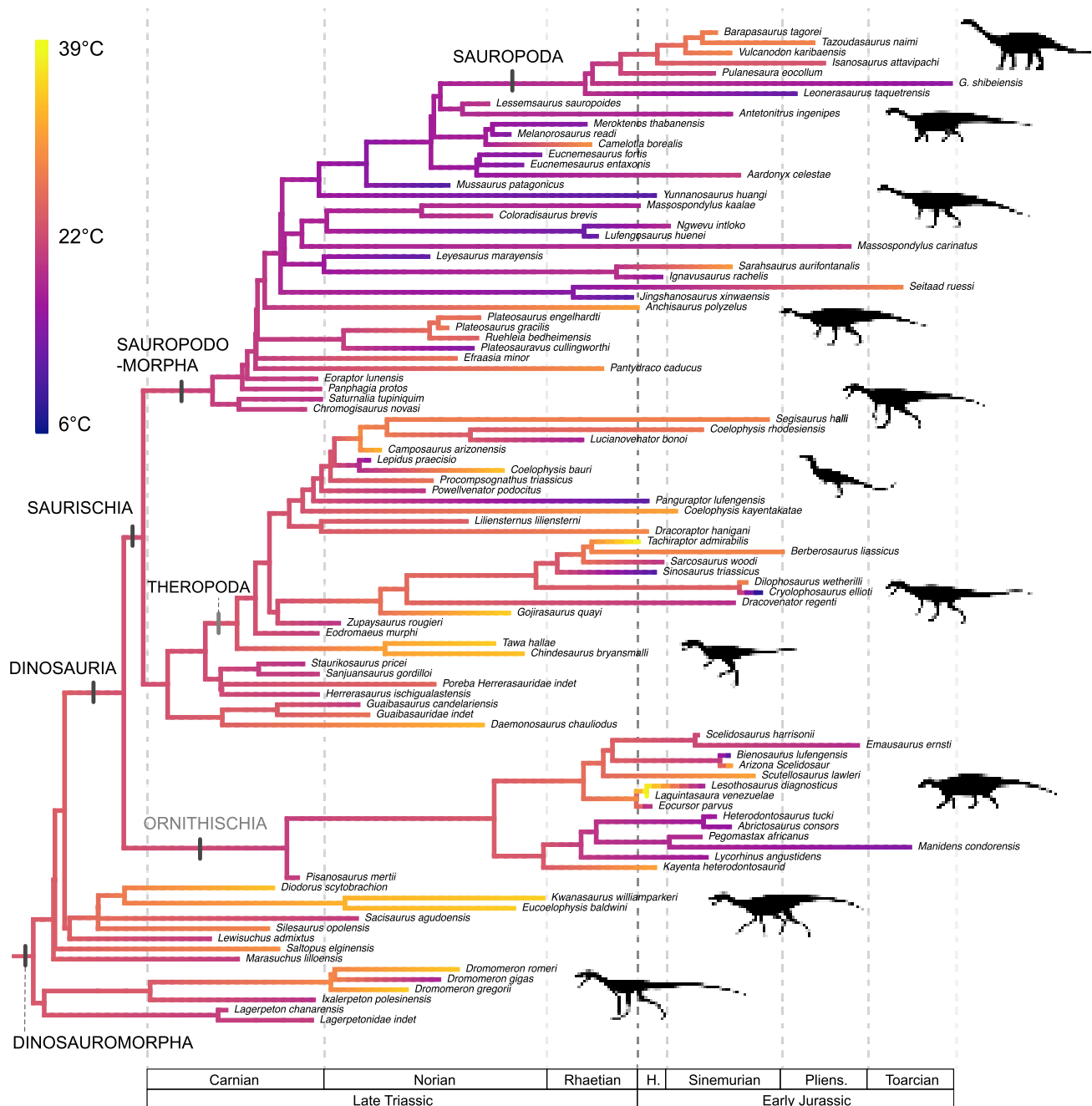


**Figure 3. Evolution of early dinosaur climate niche space**

MAT mapped as a continuous character onto a single example of the early dinosaur tree using the sauropodomorph topology of Chappelle et al.<sup>22</sup> Note that in this tree, polytomies have been randomly resolved as detailed in the STAR Methods. During the early divergences of sauropodomorphs in the Late Triassic, inferred climatic niches are “cooler.” By contrast, in the Early Jurassic, *Sarhsaurus*, *Seitaad*, and sauropods have “warmer” climatic niches. See Figure S2 for example of sauropodomorph topology of McPhee et al.<sup>23</sup> Timescale abbreviations: H., Hettangian; Pliens., Pliensbachian. Silhouettes from [phylopic.org](https://www.phylopic.org) (see acknowledgments for creator credits). See also Figure S2.

which there is no difference in evolution of their respective climatic niche between the Late Triassic and Early Jurassic (median AICc weight = 0.35; Figure 4A). This received approximately twice the support of a uniform Ornstein-Uhlenbeck (i.e., constrained) process (OU1; median AICc weight = 0.19; median  $\alpha = 0.017$ ) and three times the AICc weight of the best-supported

non-uniform model: a two-regime Ornstein-Uhlenbeck (i.e., constrained; median  $\alpha = 0.016$ ) “OUM” process with different climate optima in the Late Triassic (median  $\theta_{\text{Triassic}} = 22.024$ ) and Early Jurassic (median  $\theta_{\text{Jurassic}} = 42.578$ ; median AICc weight for OUM = 0.11). Support for a single-regime model of sauropodomorph climatic niche space evolution suggests that

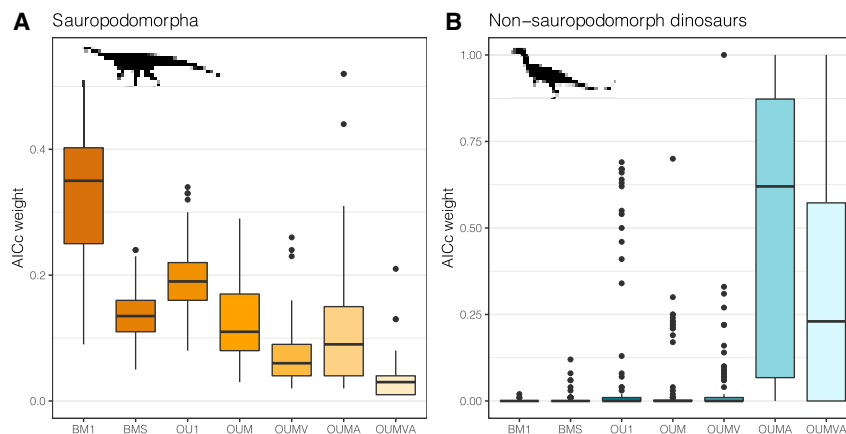


**Figure 4. Evolutionary model-fitting analysis results**

(A and B) AICc weights for evolutionary model-fitting analysis using MAT involving (A) Sauropodomorpha (Chapelle et al.<sup>22</sup> topology) and (B) non-sauropodomorph dinosaurs. Higher AICc weight values indicate greater support. Abbreviations: models beginning “BM” indicate Brownian motion, and those beginning “OU” indicate Ornstein-Uhlenbeck; for full list, see [Table S3](#). Silhouettes from [phylopic.org](#) (see [acknowledgments](#) for creator credits). See also [Figure S3](#).

they conserved their climatic niche over the Triassic-Jurassic transition in spite of changing global climate distributions that would give rise to an apparent shift if the group’s distribution was independent of climate. Support for a BM1 (diffusive) model over an OU1 (constrained) model suggests the potential for some expansion of the sauropodomorph climatic niche during this interval.

In contrast, non-sauropodomorph dinosaurs, which we use as a taphonomic control for sauropodomorph distributions, show strong evidence for an apparent shift in their climatic niche between the Late Triassic and Early Jurassic based on very high AICc weights returned for two-regime Ornstein-Uhlenbeck models ([Figure 4B](#)), especially for the OUMA model with different climatic niche optimum ( $\theta$ ) and strength of constraint ( $\alpha$ ) between the two intervals (median  $\theta_{\text{Triassic}}$  = 25.429, median  $\alpha_{\text{Triassic}}$  = 0.0148; median  $\theta_{\text{Jurassic}}$  = 20.555, median  $\alpha_{\text{Jurassic}}$  = 3.813). We describe this shift as an “apparent” shift because shifts in the distribution of climate values for a group are to be expected given changes in the global climate distribution, even if the geographic distribution of group occurrences is independent of climate; i.e., if the members of a group occupy a wide range of different climatic niches, then we expect them to be found in most or all regions, and apparent differences in niche space may result solely from variation in the prevalence of different climate zones at different points in time or from the extent to which different climate zones have been sampled in the fossil record. We interpret that as being the most likely explanation for the shifting climate distribution of non-sauropodomorph dinosaurs given that their distribution essentially tracks that of all tetrapods ([Figures 2A and 2C](#)).

This shift in the climatic niche of non-sauropodomorph dinosaurs from the Late Triassic to Early Jurassic likely reflects global changes in climate distributions through this interval and perhaps also a general northward shift in northern hemisphere fossil record sampling through the same interval.<sup>24</sup> The shift occurs despite overall fewer well-sampled fossil assemblages in the Early Jurassic when compared to the Late Triassic, which might be expected to make climatic regimes more distinct if the signal were driven by spatial variation in sampling alone. The lack of support for a shift in evolutionary regime for sauropodomorphs indicates that overall climatic niches for the group remained generally similar, in spite of shifting global climate

distributions, and that the increases in the paleogeographic range, abundance, and phenotypic diversity of sauropodomorphs primarily reflect an Early Jurassic expansion of climatic conditions favorable to the group. Framed in terms of classic hypotheses about early dinosaur evolution, these results are consistent with the idea of an “opportunistic” dinosaur expansion in response to changing environmental conditions.<sup>1,4,8</sup>

#### Late Triassic climatic restrictions on sauropodomorph distributions

During the Late Triassic, sauropodomorphs were apparently absent from lower paleolatitudes in North America and northern Africa, despite intensive sampling of key North American regions in particular ([Figure S4](#)). Paleoenvironmental studies have shown that low-paleolatitude regions during the Late Triassic experienced strong environmental fluctuations, characterized by recurring arid and humid extremes and accentuated by frequent wildfire activity and periods of drought.<sup>9,25</sup> Hypotheses for the absence of sauropodomorphs from these regions propose that they were subject to unstable environmental conditions, which may have limited food resources for large herbivores.<sup>9,25</sup> A recent study that utilized biophysical modeling suggested that heat stress may have been a limiting factor for early sauropodomorph distribution,<sup>11</sup> while others concluded that the northward dispersal of sauropodomorphs from Gondwana during the Late Triassic was likely facilitated by the lowering of climate barriers in low-latitude regions.<sup>14,15</sup>

Our results suggest that the paleogeographic restriction of Late Triassic sauropodomorphs to mid and high latitudes reflects an occupation of more restricted climatic conditions than other Late Triassic tetrapods, including theropod dinosaurs. Late Triassic sauropodomorphs occurred within a relatively narrow range of climatic conditions, characterized in particular by relatively cool MATs. These results reinforce the hypothesis that low-latitude climatic conditions acted as a barrier to sauropodomorph distribution during the Late Triassic.<sup>2,9,14,15</sup>

However, the precise reasons why sauropodomorphs in particular were apparently unable to enter warm, low-latitude regions in the Late Triassic, while theropod dinosaurs occurred over a significantly broader range of climatic conditions, remain unclear. Some form of competitive exclusion by contemporary herbivorous pseudosuchians cannot be ignored, given that pseudosuchians were most abundant and diverse at low paleolatitudes throughout their

evolutionary history.<sup>20,26</sup> However, both the impact of low-latitude environmental instability on floral communities<sup>9</sup> and physiological constraints<sup>11</sup> are worthy of further investigation.

### Early Jurassic geographic expansion of sauropodomorphs

The expansion of sauropodomorphs into lower-latitude assemblages of the Early Jurassic has remained largely unexplained by previous studies focusing on Late Triassic dinosaur distributions. Dinosaurs became considerably more abundant in the Early Jurassic following the end-Triassic mass extinction event,<sup>9,27</sup> which was brought about by global environmental change induced by major volcanism associated with emplacement of the central Atlantic magmatic province.<sup>28–31</sup> Dinosaurs exhibited high rates of survival, whereas many other large-bodied land vertebrates became extinct.<sup>1,5</sup> In particular, sauropodomorph dinosaurs increased in geographic range and abundance across the Triassic to Jurassic transition, although without associated increases in morphological disparity.<sup>32</sup>

Our results show that the Early Jurassic is marked by a broadening of the MAT conditions under which sauropodomorphs occurred. The majority of these occurrences are at cooler temperatures than known from the Late Triassic (Figures 2A and 2C), yet sauropodomorphs in both the Late Triassic and Early Jurassic show similar bounds on their overall MAT distribution (Figures 2A and 2C). Other climatic variables for sauropodomorphs are also similar between the Late Triassic and Early Jurassic, with sauropodomorphs continuing to occur, for example, most commonly in areas with strong seasonal variation in climate. Evolutionary model-fitting analyses provide further support that sauropodomorphs conserved their climatic niche from the Late Triassic to Early Jurassic.

Previous studies have suggested that sauropodomorphs—or early dinosaurs in general—were adapted to a cooler climatic niche.<sup>9,16</sup> Our analyses provide direct statistical evidence for this in sauropodomorphs. This was likely enabled by a suite of physiological, structural, and behavioral adaptations that remain unknown but may include the presence of an insulating integument, inherited from the ancestry of dinosaurs and pterosaurs (but see also Campione et al.<sup>33</sup>).<sup>16</sup> The presence of this insulating integument may have resulted in early dinosaurs having a higher tolerance of cool temperatures, resulting in niche differences between them and pseudosuchians.<sup>16</sup>

### The origins of a warm climatic niche in sauropod dinosaurs

Sauropods, the major subgroup of sauropodomorphs that persisted from the Early Jurassic to the end of the Mesozoic, were excluded from cooler climate regions at high paleolatitudes, unlike other dinosaurs.<sup>34,35</sup> This contrasts with our results for earlier sauropodomorphs, which were excluded from warmer climate regions. Phylogenetic mapping in our study indicates that the shift towards warmer climatic niches occurred around the base of Sauropoda, documenting an important shift in climatic niche synchronous with major phenotypic changes involved in sauropod origins.<sup>32,36</sup>

The extent to which this change in climatic niche is related to features such as giant adult body size and highly accelerated

growth rates<sup>37</sup> is not currently known but may be important in understanding sauropod biology. For example, bone histology indicates that sauropods underwent sustained year-round growth, contrasting with cyclical, seasonally interrupted growth in other sauropodomorphs,<sup>36–38</sup> and some authors have suggested that this may have resulted from the presence of mammal-like endothermic homeothermy in the group.<sup>37</sup> However, allometry of maximum growth rates suggests that sauropods had intermediate metabolic rates consistent with those of other dinosaurs,<sup>39,40</sup> in which case sauropods may have had a non-homeothermic (i.e., poikilothermic) metabolism and achieved sustained growth via dependence on warm environments.<sup>35</sup> We do not provide evidence that may distinguish between these different hypotheses of sauropod physiology, but we do show that an important transition in climatic niche occurred close to the origin of the group.

### Conclusions

We find that early diverging sauropodomorphs of the Late Triassic and earliest Jurassic were characterized by a cooler climatic niche. Later in the Early Jurassic, close to the radiation of Sauropoda, they shifted to a warmer niche. These results provide the first support from quantitative global climate models for climatic constraints on the early evolution of sauropodomorph dinosaurs and further demonstrate the role of environmental changes during the Triassic to Jurassic transition in driving the ecological ascendancy of dinosaurs. Unresolved questions around early dinosaur biogeography represent an avenue for future research. One such example is the apparent absence of ornithischians in the Triassic fossil record, which could reflect a climatic or paleoenvironmental control on their distribution during this interval or incorrect phylogenetic placement.<sup>41,42</sup> We provide the first insights into the timing of a major shift in climatic niche that occurred around the origins of Sauropoda and likely constrained their evolution and distribution for the remainder of the Mesozoic. Our combination of paleogeographical information on fossil distribution, spatially explicit general climate models, and evolutionary tree-based statistical analyses provides a general framework that can be used to test other key hypotheses about the influence of climate on major patterns of dinosaur evolution.

### STAR★METHODS

Detailed methods are provided in the online version of this paper and include the following:

- [KEY RESOURCES TABLE](#)
- [RESOURCE AVAILABILITY](#)
  - Lead contact
  - Materials availability
  - Data and code availability
- [EXPERIMENTAL MODEL AND SUBJECT DETAILS](#)
  - Fossil occurrence data
- [METHOD DETAILS](#)
  - Palaeoclimatic reconstructions
  - Supertree and time calibration
- [QUANTIFICATION AND STATISTICAL ANALYSIS](#)

- Principal component analysis
- Evolutionary model analysis

### SUPPLEMENTAL INFORMATION

Supplemental information can be found online at <https://doi.org/10.1016/j.cub.2022.11.064>.

### ACKNOWLEDGMENTS

We thank all contributors to the Paleobiology Database Late Triassic and Early Jurassic tetrapod occurrence data, particularly Matthew Carrano. This is Paleobiology Database publication number 445. We sincerely thank Kimberley Chapelle, Alfio Alessandro Chiarenza, Davide Foffa, Stephan Lautenschlager, Phillip Mannion, and Omar Regalado Fernandez for lending their taxonomic expertise and engaging in discussions and constructive feedback. We also thank three anonymous reviewers for invaluable comments that greatly improved the manuscript. We thank Roberto Diaz Sibaja, Tasman Dixon, and Scott Hartman for creating silhouettes and uploading them to [phylopic.org](https://phylopic.org) (CC BY 3.0 license). This research was initially funded by the European Union's Horizon 2020 research and innovation program under grant agreement 637483 (ERC starting grant TERRA to R.J.B.), and its completion was supported by a Leverhulme Research Project grant (RPG-2019-365). P.L.G. was supported by the National Science Foundation (NSF DEB 1754596) and São Paulo Research Foundation (FAPESP 2022/05697-9). A.F., P.J.V., and D.J.L. acknowledge NE/P013805/1. A.F. also acknowledges the Chinese Academy of Sciences Visiting Professorship for Senior International Scientists grant no. 2021FSE0001.

### AUTHOR CONTRIBUTIONS

E.M.D., A.F., R.B.J.B., S.E.G., and R.J.B. designed the research; E.M.D., A.F., P.L.G., and R.B.J.B. performed research and analyzed data; D.J.L. and P.J.V. contributed to the experimental design of the GCMs; E.M.D., R.B.J.B., and R.J.B. wrote the paper with contributions from all authors.

### DECLARATION OF INTERESTS

The authors declare no competing interests.

### INCLUSION AND DIVERSITY

One or more of the authors of this paper self-identifies as a gender minority in their field of research. While citing references scientifically relevant for this work, we also actively worked to promote gender balance in our reference list. We support inclusive, diverse, and equitable conduct of research.

Received: June 23, 2022

Revised: November 21, 2022

Accepted: November 28, 2022

Published: December 16, 2022

### REFERENCES

1. Brusatte, S.L., Benton, M.J., Ruta, M., and Lloyd, G.T. (2008). The first 50 Myr of dinosaur evolution: macroevolutionary pattern and morphological disparity. *Biol. Lett.* 4, 733–736. <https://doi.org/10.1098/rsbl.2008.0441>.
2. Irmis, R.B. (2010). Evaluating hypotheses for the early diversification of dinosaurs. *Earth Environ. Sci. Trans. R. Soc. Edinb.* 101, 397–426. <https://doi.org/10.1017/S1755691011020068>.
3. Benton, M.J., Forth, J., and Langer, M.C. (2014). Models for the rise of the dinosaurs. *Curr. Biol.* 24, R87–R95. <https://doi.org/10.1016/j.cub.2013.11.063>.
4. Brusatte, S.L., Benton, M.J., Ruta, M., and Lloyd, G.T. (2008). Superiority, competition, and opportunism in the evolutionary radiation of dinosaurs. *Science* 321, 1485–1488. <https://doi.org/10.1126/science.1161833>.
5. Langer, M.C., Ezcurra, M.D., Bittencourt, J.S., and Novas, F.E. (2010). The origin and early evolution of dinosaurs. *Biol. Rev. Camb. Philos. Soc.* 85, 55–110. <https://doi.org/10.1111/j.1469-185X.2009.00094.x>.
6. Langer, M.C., and Godoy, P.L. (2022). So volcanoes created the dinosaurs? a quantitative characterization of the early evolution of terrestrial pan-aves. *Front. Earth Sci.* 10, <https://doi.org/10.3389/feart.2022.899562>.
7. Tucker, M.E., and Benton, M.J. (1982). Triassic environments, climates and reptile evolution. *Palaeogeogr. Palaeoclimatol. Palaeoecol.* 40, 361–379. [https://doi.org/10.1016/0031-0182\(82\)90034-7](https://doi.org/10.1016/0031-0182(82)90034-7).
8. Benton, M.J. (1983). Dinosaur success in the triassic: a noncompetitive ecological model. *Q. Rev. Biol.* 58, 29–55.
9. Whiteside, J.H., Lindström, S., Irmis, R.B., Glasspool, I.J., Schaller, M.F., Dunlavey, M., Nesbitt, S.J., Smith, N.D., and Turner, A.H. (2015). Extreme ecosystem instability suppressed tropical dinosaur dominance for 30 million years. *Proc. Natl. Acad. Sci. USA* 112, 7909–7913. <https://doi.org/10.1073/pnas.1505252112>.
10. Bernardi, M., Gianolla, P., Petti, F.M., Mietto, P., and Benton, M.J. (2018). Dinosaur diversification linked with the Carnian pluvial episode. *Nat. Commun.* 9, 1499. <https://doi.org/10.1038/s41467-018-03996-1>.
11. Lovelace, D.M., Hartman, S.A., Mathewson, P.D., Linzmeier, B.J., and Porter, W.P. (2020). Modeling Dragons: using linked mechanistic physiological and microclimate models to explore environmental, physiological, and morphological constraints on the early evolution of dinosaurs. *PLoS One* 15, e0223872. <https://doi.org/10.1371/journal.pone.0223872>.
12. Mancuso, A.C., Benavente, C.A., Irmis, R.B., and Mundil, R. (2020). Evidence for the Carnian pluvial episode in Gondwana: new multiproxy climate records and their bearing on early dinosaur diversification. *Gondwana Res.* 86, 104–125. <https://doi.org/10.1016/j.gr.2020.05.009>.
13. Mancuso, A.C., Irmis, R.B., Pedernera, T.E., Gaetano, L.C., Benavente, C.A., and Breeden III, B.T. (2022). Paleoenvironmental and biotic changes in the late triassic of Argentina: testing hypotheses of abiotic forcing at the basin scale. *Front. Earth Sci.* 10, <https://doi.org/10.3389/feart.2022.883788>.
14. Kent, D.V., and Clemmensen, L.B. (2021). Northward dispersal of dinosaurs from Gondwana to Greenland at the mid-Norian (215–212 Ma, Late Triassic) dip in atmospheric pCO<sub>2</sub>. *Proc. Natl. Acad. Sci. USA* 118, e2020778118, <https://doi.org/10.1073/pnas.2020778118>.
15. Griffin, C.T., Wynd, B.M., Muniyikwa, D., Broderick, T.J., Zondo, M., Tolan, S., Langer, M.C., Nesbitt, S.J., and Taruvinga, H.R. (2022). Africa's oldest dinosaurs reveal early suppression of dinosaur distribution. *Nature* 609, 313–319. <https://doi.org/10.1038/s41586-022-05133-x>.
16. Olsen, P., Sha, J., Fang, Y., Chang, C., Whiteside, J.H., Kinney, S., Sues, H.-D., Kent, D., Schaller, M., and Vajda, V. (2022). Arctic ice and the ecological rise of the dinosaurs. *Sci. Adv.* 8, eabo6342. <https://doi.org/10.1126/sciadv.abo6342>.
17. Shubin, N.H., and Sues, H.-D. (1991). Biogeography of early Mesozoic continental tetrapods: patterns and implications. *Paleobiology* 17, 214–230. <https://doi.org/10.1017/S0094837300010575>.
18. Ezcurra, M.D. (2010). Biogeography of Triassic tetrapods: evidence for provincialism and driven sympatric cladogenesis in the early evolution of modern tetrapod lineages. *Proc. Biol. Sci.* 277, 2547–2552. <https://doi.org/10.1098/rspb.2010.0508>.
19. Allen, B.J., Wignall, P.B., Hill, D.J., Saupe, E.E., and Dunhill, A.M. (2020). The latitudinal diversity gradient of tetrapods across the Permo-Triassic mass extinction and recovery interval. *Proc. Biol. Sci.* 287, 20201125, <https://doi.org/10.1098/rspb.2020.1125>.
20. Dunne, E.M., Farnsworth, A., Greene, S.E., Lunt, D.J., and Butler, R.J. (2021). Climatic drivers of latitudinal variation in Late Triassic tetrapod diversity. *Palaeontology* 64, 101–117. <https://doi.org/10.1111/pala.12514>.
21. Brusatte, S.L., Butler, R.J., Niedźwiedzki, G., Sulej, T., Bronowicz, R., and Satkūnas, J. (2013). First record of Mesozoic terrestrial vertebrates from Lithuania: phytosaurs (Diapsida: Archosauriformes) of probable Late Triassic age, with a review of phytosaur biogeography. *Geol. Mag.* 150, 110–122. <https://doi.org/10.1017/S0016756812000428>.



22. Chapelle, K.E.J., Barrett, P.M., Botha, J., and Choiniere, J.N. (2019). Ngwevu intloko: a new early sauropodomorph dinosaur from the Lower Jurassic Elliot Formation of South Africa and comments on cranial ontogeny in *Massospondylus carinatus*. *PeerJ* 7, e7240. <https://doi.org/10.7717/peerj.7240>.
23. McPhee, B.W., Benson, R.B.J., Botha-Brink, J., Bordy, E.M., and Choiniere, J.N. (2018). A Giant Dinosaur from the earliest jurassic of South Africa and the transition to quadrupedality in early Sauropodomorphs. *Curr. Biol.* 28, 3143–3151.e7. <https://doi.org/10.1016/j.cub.2018.07.063>.
24. Close, R.A., Benson, R.B.J., Alroy, J., Behrensmeyer, A.K., Benito, J., Carrano, M.T., Cleary, T.J., Dunne, E.M., Mannion, P.D., Uhen, M.D., and Butler, R.J. (2019). Diversity dynamics of Phanerozoic terrestrial tetrapods at the local-community scale. *Nat. Ecol. Evol.* 3, 590–597. <https://doi.org/10.1038/s41559-019-0811-8>.
25. Lindström, S., Irmis, R.B., Whiteside, J.H., Smith, N.D., Nesbitt, S.J., and Turner, A.H. (2016). Palynology of the upper Chinle Formation in northern New Mexico, U.S.A.: implications for biostratigraphy and terrestrial ecosystem change during the Late Triassic (Norian–Rhaetian). *Rev. Palaeobot. Palynol.* 225, 106–131. <https://doi.org/10.1016/j.revpalbo.2015.11.006>.
26. Mannion, P.D., Benson, R.B.J., Carrano, M.T., Tennant, J.P., Judd, J., and Butler, R.J. (2015). Climate constrains the evolutionary history and biodiversity of crocodylians. *Nat. Commun.* 6, 8438. <https://doi.org/10.1038/ncomms9438>.
27. Olsen, P.E., Kent, D.V., Sues, H.-D., Koeberl, C., Huber, H., Montanari, A., Rainforth, E.C., Fowell, S.J., Szajna, M.J., and Hartline, B.W. (2002). Ascent of dinosaurs linked to an Iridium anomaly at the triassic-jurassic boundary. *Science* 296, 1305–1307. <https://doi.org/10.1126/science.1065522>.
28. Ruhl, M., Bonis, N.R., Reichart, G.-J., Sinninghe Damsté, J.S., and Kürschner, W.M. (2011). Atmospheric carbon injection linked to end-Triassic mass extinction. *Science* 333, 430–434. <https://doi.org/10.1126/science.1204255>.
29. Greene, S.E., Martindale, R.C., Ritterbush, K.A., Bottjer, D.J., Corsetti, F.A., and Berelson, W.M. (2012). Recognising ocean acidification in deep time: an evaluation of the evidence for acidification across the Triassic–Jurassic boundary. *Earth Sci. Rev.* 113, 72–93. <https://doi.org/10.1016/j.earscirev.2012.03.009>.
30. Davies, J.H.F.L., Marzoli, A., Bertrand, H., Youbi, N., Ernesto, M., and Schaltegger, U. (2017). End-Triassic mass extinction started by intrusive CAMP activity. *Nat. Commun.* 8, 15596. <https://doi.org/10.1038/ncomms15596>.
31. Percival, L.M.E., Ruhl, M., Hesselbo, S.P., Jenkyns, H.C., Mather, T.A., and Whiteside, J.H. (2017). Mercury evidence for pulsed volcanism during the end-Triassic mass extinction. *Proc. Natl. Acad. Sci. USA* 114, 7929–7934. <https://doi.org/10.1073/pnas.1705378114>.
32. Apaldetti, C., Pol, D., Ezcurra, M.D., and Martínez, R.N. (2021). Sauropodomorph evolution across the Triassic–Jurassic boundary: body size, locomotion, and their influence on morphological disparity. *Sci. Rep.* 11, 22534. <https://doi.org/10.1038/s41598-021-01120-w>.
33. Campione, N.E., Barrett, P.M., and Evans, D.C. (2020). On the ancestry of feathers in Mesozoic Dinosaurs. In *The Evolution of Feathers: From Their Origin to the Present Fascinating Life Sciences*, C. Foth, and O.W.M. Rauhut, eds. (Springer International Publishing), pp. 213–243. [https://doi.org/10.1007/978-3-030-27223-4\\_12](https://doi.org/10.1007/978-3-030-27223-4_12).
34. Mannion, P.D., Benson, R.B.J., Upchurch, P., Butler, R.J., Carrano, M.T., and Barrett, P.M. (2012). A temperate palaeodiversity peak in Mesozoic dinosaurs and evidence for Late Cretaceous geographical partitioning. *Glob. Ecol. Biogeogr.* 21, 898–908. <https://doi.org/10.1111/j.1466-8238.2011.00735.x>.
35. Chiarenza, A.A., Mannion, P.D., Farnsworth, A., Carrano, M.T., and Varela, S. (2022). Climatic constraints on the biogeographic history of Mesozoic dinosaurs. *Curr. Biol.* 32, 570–585.e3. [0.1016/j.cub.2021.11.061](https://doi.org/10.1016/j.cub.2021.11.061).
36. Apaldetti, C., Martínez, R.N., Cerda, I.A., Pol, D., and Alcober, O. (2018). An early trend towards gigantism in Triassic sauropodomorph dinosaurs. *Nat. Ecol. Evol.* 2, 1227–1232. <https://doi.org/10.1038/s41559-018-0599-y>.
37. Sander, P.M., Christian, A., Clauss, M., Fehner, R., Gee, C.T., Griebeler, E.-M., Gunga, H.-C., Hummel, J., Mallison, H., Perry, S.F., et al. (2011). Biology of the sauropod dinosaurs: the evolution of gigantism. *Biol. Rev. Camb. Philos. Soc.* 86, 117–155. <https://doi.org/10.1111/j.1469-185X.2010.00137.x>.
38. Botha, J., Choiniere, J.N., and Benson, R.B.J. (2022). Rapid growth preceded gigantism in sauropodomorph evolution. *Curr. Biol.* 32, 4501–4507.e2. <https://doi.org/10.1016/j.cub.2022.08.031>.
39. Grady, J.M., Enquist, B.J., Dettweiler-Robinson, E., Wright, N.A., and Smith, F.A. (2014). Evidence for mesothermy in dinosaurs. *Science* 344, 1268–1272. <https://doi.org/10.1126/science.1253143>.
40. Erickson, G.M., Rauhut, O.W.M., Zhou, Z., Turner, A.H., Inouye, B.D., Hu, D., and Norell, M.A. (2009). Was dinosaurian physiology inherited by birds? reconciling slow growth in archaeopteryx. *PLoS One* 4, e7390. <https://doi.org/10.1371/journal.pone.0007390>.
41. Agnolín, F.L., and Rozadilla, S. (2017). Phylogenetic reassessment of *Pisanosaurus mertii* Casamiquela, 1967, a basal dinosauriform from the Late Triassic of Argentina. *J. Syst. Palaeontol.* 16, 853–879. <https://doi.org/10.1080/14772019.2017.1352623>.
42. Müller, R.T., and Garcia, M.S. (2022). Oldest dinosauriform from South America and the early radiation of dinosaur precursors in Gondwana. *Gondwana Res.* 107, 42–48. <https://doi.org/10.1016/j.gr.2022.02.010>.
43. R Core Team (2021). R: A language and environment for statistical computing (R Found. Stat. Comput.). <https://www.R-Project.org>.
44. Valdes, P.J., Armstrong, E., Badger, M.P.S., Bradshaw, C.D., Bragg, F., Crucifix, M., Davies-Barnard, T., Day, J.J., Farnsworth, A., Gordon, C., et al. (2017). The BRIDGE HadCM3 family of climate models: HadCM3@Bristol v1.0. *Geosci. Model Dev. (GMD)* 10, 3715–3743. <https://doi.org/10.5194/gmd-10-3715-2017>.
45. Cox, M.D. (1984). *A Primitive Equation, 3-Dimensional Model of the Ocean: GFDL Ocean Group Technical Report No. 1* (Geophysical Fluid Dynamics Laboratory / NOAA).
46. Cox, P.M., Betts, R.A., Bunton, C.B., Essery, R.L.H., Rowntree, P.R., and Smith, J. (1999). The impact of new land surface physics on the GCM simulation of climate and climate sensitivity. *Clim. Dyn.* 15, 183–203. <https://doi.org/10.1007/s003820050276>.
47. Kiehl, J.T., and Shields, C.A. (2013). Sensitivity of the Palaeocene–Eocene Thermal Maximum climate to cloud properties. *Philos. Trans. A Math. Phys. Eng. Sci.* 371, 20130093. <https://doi.org/10.1098/rsta.2013.0093>.
48. Sagoo, N., Valdes, P., Flecker, R., and Gregoire, L.J. (2013). The Early Eocene equable climate problem: can perturbations of climate model parameters identify possible solutions? *Philos. Trans. A Math. Phys. Eng. Sci.* 371, 20130123. <https://doi.org/10.1098/rsta.2013.0123>.
49. Scotese, C.R., and Wright, N. (2018). PALEOMAP paleodigital elevation models (PaleoDEMS) for the Phanerozoic PALEOMAP Project. <https://www.earthbyte.org/paleodem-resource-scotese-and-wright-2018>.
50. Maddison, W.P., and Maddison, D.R. (2021). Mesquite: a modular system for evolutionary analysis. Version 3.70. <http://www.mesquiteproject.org>.
51. Nesbitt, S.J. (2011). The early evolution of archosaurs: relationships and the origin of major clades. *Bull. Am. Mus. Nat. Hist.* 352, 1–292.
52. Langer, M.C., Nesbitt, S.J., Bittencourt, J.S., and Irmis, R.B. (2013). Non-dinosaurian Dinosauriforms. *Geol. Soc. Lond. Spec. Publ.* 379, 157–186. <https://doi.org/10.1144/SP379.9>.
53. Martz, J.W., and Small, B.J. (2018). Non-dinosaurian dinosauriforms from the Chinle Formation (Upper Triassic) of the Eagle Basin, northern Colorado: *Dromomeron romeri* (Lagerpetidae) and a new taxon, *Kwanasaurus williamparkeri* (Silesauridae). *PeerJ* 7, e7551.
54. Butler, R.J., Upchurch, P., and Norman, D.B. (2008). The phylogeny of the ornithischian dinosaurs. *J. Syst. Palaeontol.* 6, 1–40. <https://doi.org/10.1017/S1477201907002271>.
55. Sereno, P. (2012). Taxonomy, morphology, masticatory function and phylogeny of heterodontosaurid dinosaurs. *ZooKeys* 226, 101–225.

56. Ezcurra, M.D., Butler, R.J., Maidment, S.C.R., Sansom, I.J., Meade, L.E., and Radley, J.D. (2020). A revision of the early neotheropod genus *Sarcosaurus* from the Early Jurassic (Hettangian–Sinemurian) of central England. *Zool. J. Linn. Soc.* *191*, 113–149. <https://doi.org/10.1093/zoolinnean/zlaa054>.
57. Stadler, T. (2010). Sampling-through-time in birth–death trees. *J. Theor. Biol.* *267*, 396–404. <https://doi.org/10.1016/j.jtbi.2010.09.010>.
58. Heath, T.A., Huelsenbeck, J.P., and Stadler, T. (2014). The fossilized birth–death process for coherent calibration of divergence-time estimates. *Proc. Natl. Acad. Sci. USA* *111*, E2957–E2966. <https://doi.org/10.1073/pnas.1319091111>.
59. Zhang, C., Stadler, T., Klopstein, S., Heath, T.A., and Ronquist, F. (2016). Total-Evidence Dating under the Fossilized Birth–Death Process. *Syst. Biol.* *65*, 228–249. <https://doi.org/10.1093/sysbio/syv080>.
60. Godoy, P.L., Benson, R.B.J., Bronzati, M., and Butler, R.J. (2019). The multi-peak adaptive landscape of crocodylomorph body size evolution. *BMC Evol. Biol.* *19*, 167. <https://doi.org/10.1186/s12862-019-1466-4>.
61. Ronquist, F., Teslenko, M., van der Mark, P., Ayres, D.L., Darling, A., Höhna, S., Larget, B., Liu, L., Suchard, M.A., and Huelsenbeck, J.P. (2012). MrBayes 3.2: efficient Bayesian phylogenetic inference and model choice across a large model space. *Syst. Biol.* *61*, 539–542. <https://doi.org/10.1093/sysbio/sys029>.
62. Bapst, D.W. (2012). paleotree: an R package for paleontological and phylogenetic analyses of evolution. *Methods Ecol. Evol.* *3*, 803–807. <https://doi.org/10.1111/j.2041-210X.2012.00223.x>.
63. Ezcurra, M.D., and Butler, R.J. (2018). The rise of the ruling reptiles and ecosystem recovery from the Permo-Triassic mass extinction. *Proc. Biol. Sci.* *285*, 20180361, <https://doi.org/10.1098/rspb.2018.0361>.
64. Hervé, M. (2021). RVAideMemoire: Testing and Plotting Procedures for Biostatistics (CRAN).
65. Revell, L.J. (2012). phytools: an R package for phylogenetic comparative biology (and other things). *Methods Ecol. Evol.* *3*, 217–223.
66. Beaulieu, J.M., and O’Meara, B. (2021). OUwie: Analysis of Evolutionary Rates in an OU Framework (CRAN).
67. Felsenstein, J. (1985). Phylogenies and the comparative method. *Am. Nat.* *125*, 1–15.
68. Hunt, G., and Carrano, M.T. (2010). Models and methods for analyzing phenotypic evolution in lineages and clades. *Paleontol. Soc. Pap.* *16*, 245–269. <https://doi.org/10.1017/S1089332600001893>.
69. Slater, G.J. (2013). Phylogenetic evidence for a shift in the mode of mammalian body size evolution at the Cretaceous–Palaeogene boundary. *Methods Ecol. Evol.* *4*, 734–744. <https://doi.org/10.1111/2041-210X.12084>.
70. Butler, M.A., and King, A.A. (2004). Phylogenetic comparative analysis: a modeling approach for adaptive evolution. *Am. Nat.* *164*, 683–695. <https://doi.org/10.1086/426002>.
71. Benson, R.B.J., Hunt, G., Carrano, M.T., and Campione, N. (2018). Cope’s rule and the adaptive landscape of dinosaur body size evolution. *Palaeontology* *61*, 13–48. <https://doi.org/10.1111/pala.12329>.
72. Hurvich, C.M., and Tsai, C.-L. (1989). Regression and time series model selection in small samples. *Biometrika* *76*, 297–307. <https://doi.org/10.1093/biomet/76.2.297>.
73. Burnham, K.P., and Anderson, D.R. (2002). *Model Selection and Multimodel Inference* (Springer).

## STAR★METHODS

### KEY RESOURCES TABLE

RESOURCE or REAGENT	SOURCE	IDENTIFIER
<b>Data</b>		
Paleobiology Database	<a href="https://paleobiodb.org">https://paleobiodb.org</a>	accessed May 2022
Paleoclimate reconstructions (HadCM3L)	<a href="http://www.bridge.bris.ac.uk/resources/simulations">http://www.bridge.bris.ac.uk/resources/simulations</a>	accessed June 2022
Deposited data	This paper	Available via the Open Science Framework at <a href="https://doi.org/10.17605/OSF.IO/VRZ74">https://doi.org/10.17605/OSF.IO/VRZ74</a>
Supertree	This paper	Available via the Open Science Framework at <a href="https://doi.org/10.17605/OSF.IO/VRZ74">https://doi.org/10.17605/OSF.IO/VRZ74</a>
<b>Software and algorithms</b>		
R computing environment	<a href="http://www.R-project.org">http://www.R-project.org</a>	Version 4.0.5
Deposited code	This paper	Available via the Open Science Framework at <a href="https://doi.org/10.17605/OSF.IO/VRZ74">https://doi.org/10.17605/OSF.IO/VRZ74</a>
Mesquite	<a href="https://www.mesquiteproject.org">https://www.mesquiteproject.org</a>	Version 3.70
MrBayes: Bayesian Inference of Phylogeny	<a href="https://nbisweden.github.io/MrBayes/download.html">https://nbisweden.github.io/MrBayes/download.html</a>	Version 3.2
paleotree R package	<a href="https://cran.r-project.org/web/packages/paleotree/index.html">https://cran.r-project.org/web/packages/paleotree/index.html</a>	Version 3.4.5
RVAideMemoire R package	<a href="https://cran.r-project.org/web/packages/RVAideMemoire/index.html">https://cran.r-project.org/web/packages/RVAideMemoire/index.html</a>	Version 0.9.81.2
phytools R package	<a href="https://cran.r-project.org/web/packages/phytools/index.html">https://cran.r-project.org/web/packages/phytools/index.html</a>	Version 1.2.0
OUwie R package	<a href="https://cran.r-project.org/web/packages/OUwie/index.html">https://cran.r-project.org/web/packages/OUwie/index.html</a>	Version 2.10

### RESOURCE AVAILABILITY

#### Lead contact

Further information and requests for resources should be directed to and will be fulfilled by the lead contact, Emma Dunne ([dunne.emma.m@gmail.com](mailto:dunne.emma.m@gmail.com)).

#### Materials availability

This study did not generate new unique reagents.

#### Data and code availability

All relevant data and R code supporting our analyses are available via the Open Science Framework at <https://doi.org/10.17605/OSF.IO/VRZ74>. Palaeoclimate outputs from the HadCM3L General Circulation Model used here come from the BRIDGE group (University of Bristol) and are available at: <http://www.bridge.bris.ac.uk/resources/simulations>.

## EXPERIMENTAL MODEL AND SUBJECT DETAILS

### Fossil occurrence data

Global occurrences for Late Triassic–Early Jurassic (Carnian–Toarcian; 237–174 Ma) tetrapods were downloaded from the Paleobiology Database ([paleobiodb.org](http://paleobiodb.org)) (see [Figure S4](#)). Before download, the data were checked against the current published literature for completeness and missing occurrences identified during this vetting procedure were added. The downloaded dataset was filtered to remove trace fossils, marine and flying taxa, and taxonomically indeterminate occurrences. Data preparation and analyses were conducted within R 4.0.5.<sup>43</sup>

## METHOD DETAILS

### Palaeoclimatic reconstructions

We used a set of palaeoclimate model simulations using an updated version of the UKMO HadCM3 family, a coupled Atmosphere–Ocean General Circulation Model (AOGCM), but with a lower resolution ocean called HadCM3L (specifically HadCM3L-M2.1aD, following the nomenclature of Valdes, et al.<sup>44</sup>). The model has a resolution of 3.75° longitude × 2.5° latitude in the atmosphere and ocean, with 19 hybrid levels in the atmosphere and 20 vertical levels in the ocean with equations solved on the Arakawa B-grid with sub-grid scale processes (such as convection, clouds, and gravity wave drag) parameterised. The ocean model is that of Cox,<sup>45</sup> a fully three-dimensional, full primitive equation model. Sea-ice is calculated on a zero-layer model with partial sea ice coverage possible.

Because geological data recording land surface vegetation for Triassic–Jurassic stages are uncertain and globally sparse, we use a version of the model that includes the dynamical vegetation model TRIFFID (Top-Down Representation of Interactive Foliage and Flora Including Dynamics) and land surface scheme MOSES 2.1.<sup>46</sup> TRIFFID predicts the distribution and properties of global vegetation based on plant functional types (PFTs), in the form of fractional coverage (and thus PFT co-existence) within a grid-cell based on competition equations of climate tolerance of five plant functional types.

Our version of HadCM3L shows skill at reproducing the modern climate<sup>44</sup> and has contributed to both the Coupled Model Intercomparison Projects (CMIP) as well as Palaeoclimate Model Intercomparison Model Projects (PMIP). The model has a further update that includes modification to cloud condensation nuclei density and cloud droplet effective radius following the work of Kiehl & Shields<sup>47</sup> and Sagoo et al.<sup>48</sup> This produces warm palaeoclimate higher latitude temperatures where previous models have been found to be too cool compared to proxy-data, as well as reproducing a pre-industrial climate in good agreement with modern observations. Unlike some coupled models, HadCM3L does not require flux adjustments (through addition or subtraction of heat or salinity in the ocean) to prevent the model from drifting to unrealistic values. To fully equilibrate simulations of past time periods, especially in the deep ocean, long integration periods are required (>5000 model years). Such long integrations of the model would not be possible with higher resolution models. Overall, we consider HadCM3L an appropriate tool for this work, due to its balance of sufficient complexity and resolution to represent key climate features, and sufficient efficiency to allow the necessary long simulations.

Seven model simulations for the Carnian (233.2 Ma), Norian (222.4 Ma), Rhaetian (204.9 Ma), Hettangian (201.3 Ma), Sinemurian (196.0 Ma), Pliensbachian (186.8 Ma) and Toarcian (178.4 Ma) were carried out using stage-specific boundary conditions (topography, bathymetry, solar luminosity, continental ice,  $p\text{CO}_2$ ). Stage-specific realistic carbon dioxide concentrations were chosen based on proxy- $\text{CO}_2$  (Carnian [1613.5ppm], Norian [1810.4ppm], Rhaetian [1503.2ppm], Hettangian [1728.9ppm], Sinemurian [1783.7ppm], Pliensbachian [948.8ppm] and Toarcian [986.2ppm]) reconstructions from Foster et al. (2017). The solar constant was based on Gough (1981). Paleogeographic digital elevation models (DEMs) were reproduced from Scotese & Wright.<sup>49</sup> Each stage-specific DEM is interpolated from a 1°×1° grid onto the model 3.75°×2.5° grid. Similarly, land ice is also transformed onto the model grid assuming a simple parabolic shape to estimate the ice sheet height (m). Surface soil conditions were set at a uniform medium loam everywhere because stage specific soil parameters during the Triassic–Jurassic are unknown. All other boundary conditions (such as orbital parameters, aerosol concentrations, etc.) are held constant at pre-industrial values. A modern orbit is chosen on the basis that it has a low-eccentricity, which corresponds to a long-term orbital average. Atmospheric composition and concentration of aerosols is unknown for such deep-time periods, however future investigation through the use of an interactive aerosol scheme would offer a useful insight on their potential impact on climate. To ensure all simulations are fully equilibrated we ensure that (i) the globally and volume-integrated annual mean ocean temperature trends are less than 1°C per 1000 years, (ii) trends in surface air temperature are less than 0.3°C per 1000 years, and (iii) net energy balance at the top of the atmosphere, averaged over a 100-year period at the end of the simulation, are less than 0.25/W m<sup>2</sup>. Modelled climatological means were calculated from the last 100 years of each simulation.

For a robust comparison of model variables (e.g. temperature/precipitation) versus the proxy record we consistently rotate the modern-day proxy locations to their time-dependent grid-cell locations during the Late Triassic and Early Jurassic. To define the seasonal variation in specific variables, for example for temperature, we use the 3-warmest and 3-coldest months with a seasonal range defined as the 3-warmest months minus the 3-coldest months.

Palaeoclimatic variables were assigned to individual taxa based on their occurrences (i.e. geographic locality and stratigraphic age). Occurrences that spanned more than two geological intervals due to stratigraphic uncertainty were discarded from the dataset. Those that ranged across two intervals (e.g. Hettangian–Sinemurian), the mean was calculated for each palaeoclimatic variable. Prior to settling on this approach, palaeoclimatic variables were also assigned using a ‘randomized-averaging’ process, where

occurrences that spanned two time intervals were randomly assigned to a single one of these intervals, and this process performed over multiple iterations. The results obtained from this more complex approach remained consistent with the approach described above and presented here.

### Supertree and time calibration

An informal species-level supertree was constructed using the software Mesquite<sup>50</sup> based on the most up-to-date phylogenetic analyses available for Late Triassic–Early Jurassic dinosaurs. The interrelationships shown in the supertree reflect congruence between overlapping topologies of the source phylogenetic analyses; polytomies were generated when source phylogenies showed incongruent relationships. The overall topology broadly follows Nesbitt,<sup>51</sup> with the taxonomy of dinosauromorphs following Langer et al.<sup>52</sup> Silesaurid phylogeny follows Martz & Small,<sup>53</sup> and the position of *Pisanosaurus* is based on Agnolín & Rozadilla.<sup>41</sup> Ornithischian relationships generally follow Butler et al.,<sup>54</sup> with heterodontosaurid taxonomy and phylogeny after Sereno.<sup>55</sup> Theropod relationships (including Coelophysidae) were based on Ezcurra et al.<sup>56</sup> To accommodate uncertainties in sauropodomorph phylogeny, we constructed two alternate topologies for Late Triassic–Early Jurassic sauropodomorph relationships; one following Chapelle et al.<sup>22</sup> and the other following McPhee et al.<sup>23</sup> Each of these alternate sauropodomorph topologies was then grafted to the dinosauromorph-theropod-ornithischian section described above to make two supertrees, one containing 101 taxa (Chapelle topology) and 107 taxa (McPhee topology). Several biogeographically-important specimens that have not been identified to species level were also added to the supertree (Table S2). Six stratigraphically older archosaur taxa (*Arizonasaurus*, *Ctenosauriscus*, *Dongusuchus*, *Teleocrater*, *Xilousuchus*, and *Yarasuchus*) were also included in order to date deeper nodes.

These two topologies were used to produce time-calibrated trees, in which polytomies were randomly resolved, using the fossilised birth-death (FBD) model<sup>57–59</sup> following the protocol outlined in Godoy et al.<sup>60</sup> The FBD method is a Bayesian tip-dating approach which uses a birth-death process that includes the probability of fossilization and sampling to model the occurrence of fossil species in the phylogeny and estimate divergence times (=node ages). Information on occurrence times of all species in the supertree (=tip ages) were initially obtained from the Paleobiology Database but were then checked against primary sources in the literature to obtain the most precise age estimates available based on the geological formations within which each species occurs. An ‘empty’ character matrix for performing Bayesian Markov chain Monte Carlo (MCMC) analyses in MrBayes version 3.2,<sup>61</sup> following the protocol within the R package *paleotree*.<sup>62</sup> Supertree topologies (with alternative topologies for sauropodomorpha) were used as topological constraints and uniform priors were set on the tip ages. A uniform prior was used for the root of the trees, constrained between 255.5 and 260.4 Ma as a dinosauromorph origin older than the latest Permian is unlikely given our understanding of the early archosauromorph fossil record.<sup>63</sup> For each topology, two runs with four chains of 10,000,000 generations were used, after which the parameters indicated that both MCMC runs seemed to converge i.e. the Potential Scale Reduction Factor approached 1.0 and average standard deviation of split frequencies was below 0.01. For both topologies, 100 trees were randomly sampled from the posterior distribution after a burn-in of 25%. As our results were consistent across both alternative topologies for sauropodomorphs, we focused on the Chapelle topology for the results present here in the main text.

## QUANTIFICATION AND STATISTICAL ANALYSIS

### Principal component analysis

To explore the climatic niche space occupied by early dinosaurs and other tetrapods, we performed a principal component analysis (PCA) using the *prcomp* function in R, which included the scaling argument so that variables were scaled to have unit variance before the analysis took place. Separate PCA plots were constructed for the Late Triassic (Carnian–Rhaetian) and Early Jurassic (Hettangian–Toarcian) to explore changes through the Triassic to Jurassic transition. We also constructed boxplots to illustrate and explore the range of palaeoclimatic conditions occupied by each tetrapod group, again separated into the Late Triassic and Early Jurassic. A non-parametric multivariate analysis of variance (npMANOVA) was performed to statistically compare the distribution of the two groups using the R package *RVAideMemoire*<sup>64</sup> (Table S1). Raincloud plots were constructed to examine the range of individual palaeoclimatic conditions occupied by both groups.

### Evolutionary model analysis

We applied a model-fitting approach to characterize the evolutionary mode of early dinosaur climatic niche evolution through the Triassic–Jurassic transition. In this instance, the continuous trait was the mean annual temperature (MAT) for each early dinosaur species. Many taxa are known only from one or a handful of occurrences, meaning that within-species variation in MAT could not reasonably be estimated. Therefore, for species with multiple occurrences, we used a mean value for MAT. First, MAT was plotted onto multiple example trees using the continuous character mapping function `contMap()` in *phytools*,<sup>65</sup> in which mapping is accomplished by estimating the states at internal nodes of the tree using maximum likelihood (ML) with the function `fastAnc()` (a fast estimation of the ML ancestral states for a continuous trait) and interpolating the states along each edge).

Model-fitting analyses were carried out using the R package *OUwie*,<sup>66</sup> which allows modes of continuous character evolution to be estimated under Brownian motion and Ornstein-Uhlenbeck models.<sup>67,68</sup> As above, the continuous character in this instance was the mean annual temperature (MAT) for each early dinosaur species. Across all model-fitting analyses, we included estimates of the standard deviation associated with each MAT value. Abbreviations and definitions for all models used are listed in Table S3. Uniform models apply a single set of model parameters across all branches of a phylogeny. We fitted two uniform models: (1) A uniform

Brownian motion (BM) model, which describes diffusive, unconstrained evolution via random walks along independent phylogenetic lineages, resulting in no directional trend in trait mean, but with increasing trait variance (=disparity) through time.<sup>67–69</sup> (2) The Ornstein-Uhlenbeck (OU) model, which describes processes where a trait's variance is constrained around one or several optima often referred to as 'selective regime' or 'adaptive zone' optima at the macroevolutionary scale.<sup>69–71</sup> In addition to these uniform models, we also fitted five time-shift (non-uniform) models, also using the R package *OUwie*. First, a non-uniform Brownian motion model with different rate parameters for each state on a tree (BMS). Finally, four non-uniform Ornstein-Uhlenbeck (OU) models, three of which (OUMV, OUMA, and OUMVA) allow  $\alpha$  (the parameter that describes the strength of pull towards a central value, typically referred to as the selective optima) and  $\sigma^2$  (a constant that describes the stochastic spread of the trait values over time i.e. under a Brownian motion process) to vary, and another (OUM) that has different state means and a single  $\alpha$  and  $\sigma^2$  acting all selective regimes (see [Table S3](#)). Measurement error was incorporated using the `mserr="known"` argument of the `OUwie()` function. This provides the standard error estimates for each species mean.<sup>67</sup> Model support was compared using Akaike weights computed from small-sample-corrected AIC scores (AICc),<sup>72,73</sup> where lower AICc scores and higher AIC weights correspond to better fitting models.